Online Spatial-Temporal EV Charging Scheduling with Incentive Promotion

LO PANG-YUN TING, National Cheng Kung University, Taiwan
HUAN-YANG WANG, National Cheng Kung University, Taiwan
JHE-YUN JHANG, National Cheng Kung University, Taiwan
KUN-TA CHUANG, National Cheng Kung University, Taiwan

The growing adoption of electric vehicles (EVs) has resulted in an increased demand for public EV charging infrastructure. Currently, the collaboration between these stations has become vital for efficient charging scheduling and cost reduction. However, most existing scheduling methods primarily focus on recommending charging stations without considering users' charging preferences. Adopting these strategies may require considerable modifications to how people charge their EVs, which could lead to a reluctance to follow the scheduling plan from charging services in real-world situations. To address these challenges, we propose the *POSKID* framework in this paper. It focuses on spatial-temporal charging scheduling, aiming to recommend a feasible charging arrangement, including a charging station and a charging time slot, to each EV user while minimizing overall operating costs and ensuring users' charging satisfaction. The framework adopts an online charging mechanism that provides recommendations without prior knowledge of future electricity information or charging requests. To enhance users' willingness to accept the recommendations, *POSKID* incorporates an incentive strategy and a novel embedding method combined with Bayesian personalized analysis. These techniques reveal users' implicit charging preferences, enhancing the success probability of the charging scheduling task. Furthermore, *POSKID* integrates an online candidate arrangement selection and an explore-exploit strategy to improve the charging arrangement recommendations based on users' feedback. Experimental results using real-world datasets validate the effectiveness of *POSKID* in optimizing charging management, surpassing other strategies. The results demonstrate that *POSKID* benefits each charging station while ensuring user charging satisfaction.

CCS Concepts: • **Computing methodologies → Planning under uncertainty**; • **Information systems → Data mining**.

Additional Key Words and Phrases: Online Charging Management, Spatial-Temporal Scheduling, Online Knapsack Problem, Personalized Inference, Knowledge Graph Embedding, Reinforcement Learning

ACM Reference Format:
Lo Pang-Yun Ting, Huan-Yang Wang, Jhe-Yun Jhang, and Kun-Ta Chuang. 2023. Online Spatial-Temporal EV Charging Scheduling with Incentive Promotion. *J. ACM* 37, 4 (August 2023), 25 pages. https://doi.org/XXXXXXX.XXXXXXX

Authors' addresses: Lo Pang-Yun Ting, National Cheng Kung University, Tainan, Taiwan, lpyting@netdb.csie.ncku.edu.tw; Huan-Yang Wang, National Cheng Kung University, Tainan, Taiwan, hywang@netdb.csie.ncku.edu.tw; Jhe-Yun Jhang, National Cheng Kung University, Tainan, Taiwan, jyjhang@netdb.csie.ncku.edu.tw; Kun-Ta Chuang, National Cheng Kung University, Tainan, Taiwan, ktchuang@mail.ncku.edu.tw.

0004-5411/2023/8-ART $15.00
https://doi.org/XXXXXXX.XXXXXXX

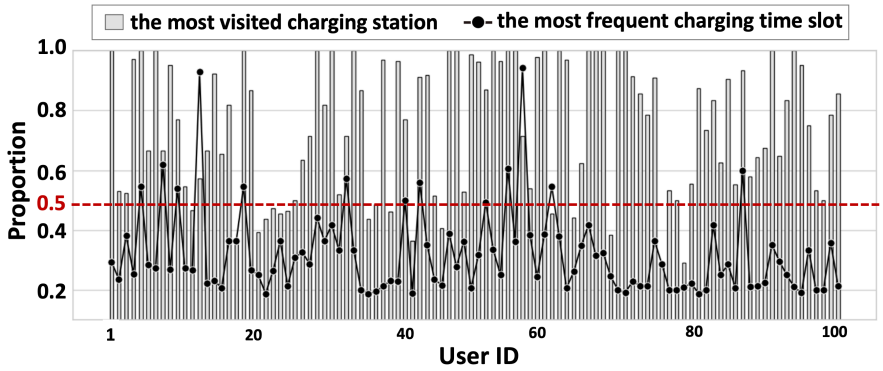

Fig. 1. The charging proportions for 100 EV users randomly chosen from Drive Dundee Electric [9]. The y-axis represents the proportion of a user's charging activities at their most visited stations and their most frequent charging time slots compared to their total number of charging records. A higher proportion indicates a user has a higher tendency to charge at a particular station or a time slot. Note that a time slot refers to a specific hour.

1 INTRODUCTION

The transition from conventional cars to electric vehicles (EVs) is an irreversible trend. The International Energy Agency (IEA) [18] predicts that the number of electric vehicles sold worldwide will exceed 14 million in 2023, representing approximately 18% of all car sales in that year [8]. Thus, the requirement for EV charging infrastructure is on the rise, prompting the development of various approaches and partnerships to satisfy this demand. A promising business opportunity is the installation of EV charging stations in retail sites. According to a financial analysis conducted by ATLAS Public Policy [30], retailers are considered as ideal operators to install EV charging stations for two main reasons. First, it provides the opportunity for customers who visit stores to use the charging stations. Second, customers waiting for their vehicles to charge tend to spend more time browsing inside the store, leading to higher retail sales in the store. Retailers can leverage these benefits not only to assist in constructing public electric vehicle charging infrastructure but also to boost their own profits and customer loyalty.

Despite this, if charging behavior is not properly managed, it may cause a detrimental impact. Typically, retailers need to sign contracts with electricity providers to specify their contracted capacity demand (the upper bound of instant electricity consumption). If the instant power consumption exceeds the contracted capacity, an additional penalty will be charged [12]. To mitigate this, several solutions have been proposed to schedule EV charging and minimize operating costs [22, 39, 42]. Nevertheless, these techniques may not be feasible in actual circumstances for two reasons: (i) most of them assume that all charging demands are already known beforehand, and (ii) these studies generally assume that all EV owners will agree to the pre-scheduled charging arrangement.

Therefore, in [38] we proposed the *POSIT* framework for the practical scheduling of EV charging in scenarios where a charging operator owns an EV charging station and a retail building. *POSIT* aims to provide a feasible schedule for various EV users while increasing the profit of the charging operator. The challenges of *POSIT* arise from how to instantly recommend the best charging schedule when each charging request comes while only considering the current energy information. In *POSIT*, an online charging scheduling approach is employed to select the most valuable charging time slots with relevant incentives to enhance the user's willingness to accept the charging recommendation. A previous study [40] has demonstrated the efficacy of both monetary and non-monetary incentives

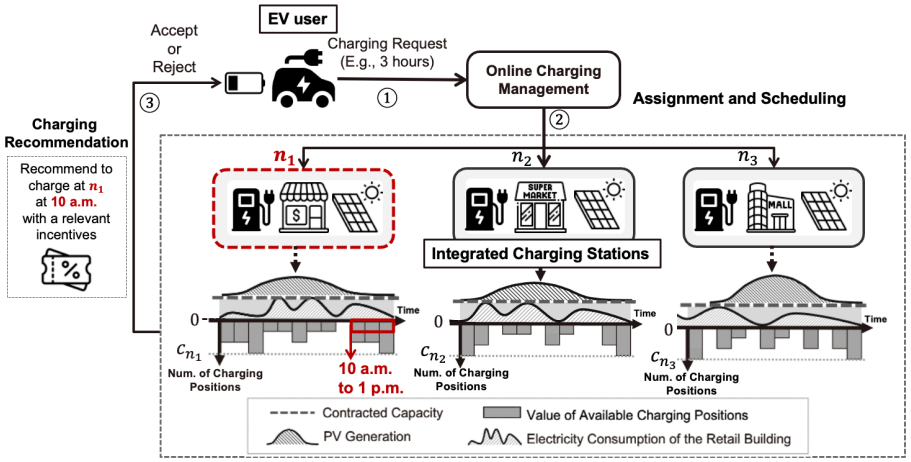

Fig. 2. This figure outlines our proposed system for online electric vehicle (EV) charging. Initially, an EV owner submits a request for charging, specifying their preferred duration, to our platform. Next, our system evaluates the current state of all charging stations (each station, denoted as n_i, is outfitted with a retail building and solar panel by default) to identify the most suitable station for the EV user. Subsequently, the user receives a recommendation for a charging station and a designated charging time, along with applicable incentives. Note that c_{n_i} represents the number of charging connectors at station n_i.

in altering EV users' charging behaviors, thereby endorsing the use of incentives in *POSIT* for optimizing charging recommendation.

However, it's important to note that *POSIT* can only apply to the single charging station to recommend charging time slots, focusing on temporal charging scheduling. As the trend of EV charging infrastructure is dramatically growing, cooperation between charging stations has become a popular business mechanism [11, 23]. This highlights the importance of spatial-temporal charging scheduling to recommend both charging time slots and charging stations for EV users. Nevertheless, these works overlook some important practical issues. ❶ Firstly, EV owners usually have their preferences for certain charging stations or time slots to charge their EVs. Our analysis of real-world EV charging data, as shown in Figure 1, reveals that some users consistently charge at the same times and their favorite particular stations, leading to unbalanced utilization between multiple stations. Inevitably, the lower utilization of less popular stations would decrease the motivation to construct charging stations, thus slowing the penetration of the charging infrastructure. ❷ Secondly, at peak time, popular charging stations often experience a surge of charging requests, resulting in an undesirable risk and penalty for exceeding the limit set in the electricity contract. In reality, such a surge in electricity demand can also lead to an unstable electric power grid [3].

Proposed Method:

To address the aforementioned issues, we propose an extension of the *POSIT* framework, called *POSKID* (**P**ersonalized **O**nline **S**cheduling with **K**nowledge-Based **I**nference into **D**ynamic Decision-Making) in this paper. *POSKID* focuses on scheduling the timing and location of charging to reduce the operating costs of charging stations by managing station utilization balance and while ensuring the satisfaction of EV users.

Specifically, in the *POSKID* system, an online service is used to suggest appropriate charging arrangements, encompassing both charging stations and charging time slots, incorporating incentive strategies within a fixed budget. Figure 2 shows how our online system works. It enables EV users

to book their desired charging duration (e.g., 3 hours) through the registration process. A retail building is connected to a charging station, which could be a form of cooperative marketing, such as offering coupons that can be used for in-store purchases or to offset charging fees for EV users. The *POSKID* framework formally offers the EV user a recommended charging station and a charging time slot, along with incentives such as coupons. The EV user can choose to either accept or decline the suggested arrangement.

In our *POSKID* system, to accommodate EV users' charging preferences, we focus on enhancing users' **W**illingness **T**o **A**ccept recommendations (abbreviated as WTA in this work). Specifically, *POSKID* not only extends the incentive mechanism used in *POSIT*, but also incorporates the following techniques to enable effective EV scheduling:

(1) A *relative knowledge graph* is designed that captures the relative relationships between multiple charging stations, and a novel knowledge graph embedding method with Bayesian analysis techniques is introduced to infer users' WTA to different charging recommendations.
(2) An online candidate arrangement selection is proposed to identify profitable charging arrangements by considering users' WTA and the utilization balance of charging stations.
(3) Interactive learning is adopted based on users' feedback to improve the scheduling process.

The design of *POSKID* offers two main benefits: (***i***) it balances utilization across stations to minimize operational expenses by both reducing electricity costs at high-demand stations without surpassing contracted capacities and enhancing income at lower-demand stations through the allocation of more charging tasks. (***ii***) it improves users' WTA using the incentive strategy, while not significantly changing their original charging habits to ensure their satisfaction. This creates a win-win situation for both charging stations and EV users, showcasing the strengths of *POSKID* in practical applications.

Contributions:

- We design an online charging spatial-temporal scheduling that recommends charging stations and charging time slots for EV users, with the goal of reducing the operating costs for all participating charging stations and ensuring EV users' satisfaction.
- To enhance EV users' willingness to accept (WTA), we employ a combination of relevant incentives and a novel embedding method with Bayesian personalized analysis. This approach is applied to the designed relative knowledge graph, allowing us to effectively learn users' implicit charging preferences and further improve the satisfaction of EV users.
- We validate the effectiveness of *POSKID* using real-world EV charging datasets. Experimental results show that *POSKID* surpasses baselines by reaching an optimal compromise between lowering overall operating costs and ensuring user satisfaction. Additionally, we also conduct an analysis to examine the individual benefits of each station under our framework.

2 PRELIMINARY

Before formally introducing the *POSKID* framework, we describe the necessary symbols and definitions. For the sake of simplicity, we assume that all EVs charge at uniform speeds*.

Definition 1 (Integrated Charging Station (ICS)): Let $\mathcal{N}$ be the set of integrated charging stations (ICSs). Each ICS, denoted as $n \in \mathcal{N}$, is equipped with solar panels and a retail building. An ICS is characterized by the following information: (i) the number of charging positions (connectors) (ii) the geographic location (latitude and longitude), and (iii) the category of the retail building (e.g., convenience store, supermarket, and so on).

*For the sake of simplicity, we assume equal charging speeds in our discussion. It is believed that the implementation issue of variant charging speeds can be seamlessly extended in *POSKID*.

Definition 2 (User Charging Record): Let $\mathcal{V}$ denote the set of EV users, where each EV user $v \in \mathcal{V}$ is associated with a set of historical charging records R^v. Each charging record $\mathrm{r}^v \in R^v$ consists of three information of user v: the arrival time t_{arr}, the departure time t_{dep}, and the charging place (ICS) n. Based on the assumption of uniform charging speeds, the energy demand for each EV is determined by the duration of charging ($t_{dep} - t_{arr}$).

Definition 3 (Charging Request): We denote $\mathrm{q} = (v, t, h)$ as a charging request submitted by EV user $v \in \mathcal{V}$ for time slot t, where $h \in \mathbb{Z}^+$ represents the required charging duration (the number of hours). Note that a time slot refers to a specific hour of the day.

Definition 4 (Ideal Available Capacity): The forecasted number of available EV charging positions in the future, referred to as "ideal available capacity", is crucial for reducing the operating costs of charging operators [38]. In our scenario of ICSs, in addition to charging demands, the primary sources of electricity generation and consumption are solar photovoltaic (PV) power generation and the energy consumption of the associated retail building. Let e_c^n represent allowable energy usage (without incurring penalties) for ICS n under its contracted capacity. In addition, $\tilde{e}_p^n(t')$ and $\tilde{e}_h^n(t')$ denote the predicted PV generation and the energy consumption of ICS n's associated retail building in time slot t', predicted using the LSTM model, respectively. The remaining energy $e_r^n(t')$ for ICS n in time slot t' is defined as follows:

$$e_r^n(t') = e_c^n + \tilde{e}_p^n(t') - \tilde{e}_h^n(t'). \tag{1}$$

Given the assumption of uniform charging speeds for all EVs, the energy charged per EV in a time slot is represented by ω. The notation c^n represents the number of charging connectors at ICS n. We define $l_{t'}^n$, the value of ideal available capacity at time slot t' for ICS n, as follows:

$$l_{t'}^n = \begin{cases} \min\left(\left\lfloor \dfrac{e_r^n(t')}{\omega} \right\rfloor, c^n \right) & , \text{if } e_r^n(t') > 0 \\ 0 & , \text{otherwise} \end{cases}, l_{t'}^n \in \mathbb{N}_0, \tag{2}$$

where $\lfloor \cdot \rfloor$ denotes the floor function, which rounds down to the nearest integer.

Definition 5 (Incentive): In our scenario, involving multiple integrated charging stations (ICSs), "incentives" are defined as coupons issued by our system and are considered monetary incentives. These coupons can be utilized for in-store purchases at ICSs or to reduce charging fees, each possessing a predetermined face value. Through the deployment of these monetary incentives, our objective is to identify which EV users to target and determine the quantity of incentives to be allocated to each, thereby encouraging users to adhere to our suggested charging arrangements. Note that once a user submits a charging request and accepts our recommendation, they become eligible to receive the corresponding incentives.

Problem Statement: For each charging request $\mathrm{q} = (v, t, h)$ submitted by EV user v in time slot t, and considering the set of ICSs $\mathcal{N}$, charging records R^v of EV user v, ideal available capacity $\{l_{t'}^n | n \in \mathcal{N}, t' > t\}$, and a fixed incentive budget B for all ICSs per day, our objective is to recommend a charging arrangement $M^v = \{n, \tau, \vartheta\}$ for EV user v's charging request q_t^v. Here n, τ, and ϑ represent the recommended ICS, the starting time slot for charging, and the amount of provided incentives, respectively. Note that for the recommended charging arrangement $M^v = \{n, \tau, \vartheta\}$, we anticipate that the charging end time slot for EV user v will be $\tau + h - 1$, based on the user's required charging duration h.

By recommending charging arrangements tailored to EV users' willingness to accept (WTA), we enhance the success rate of these recommendations. Additionally, estimating the *ideal available capacity* for future time slots aids in mitigating penalties from exceeding contracted capacities of ICSs. This approach optimizes ICS usage to minimize operating costs and ensures user satisfaction with their charging experiences.

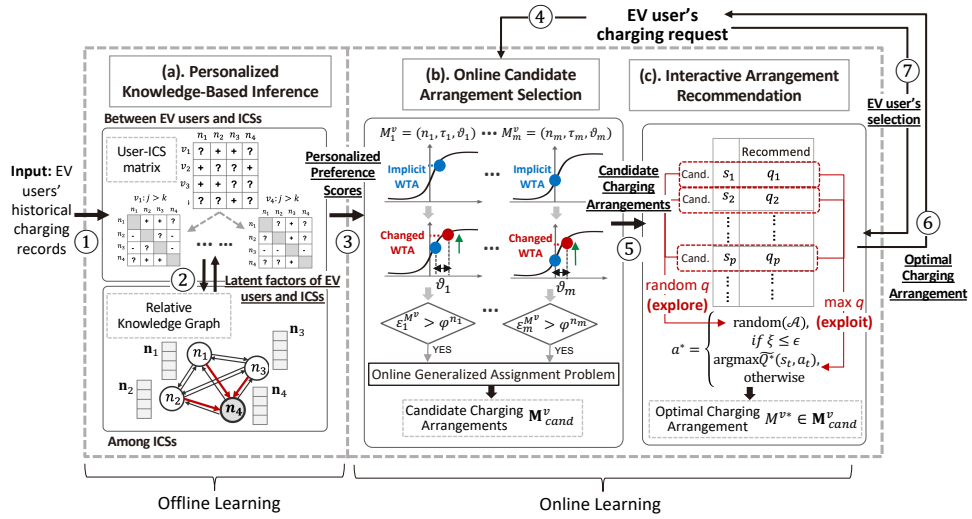

Fig. 3. The overview of *POSKID* framework

3 FRAMEWORK

In this section, we introduce the structure of the proposed *POSIKID* (**P**ersonalized **O**nline **S**cheduling with **K**nowledge-Based **I**nference into **D**ynamic Decision-Making) framework. As shown in Figure 3, the *POSKID* framework comprises three main components:

- **Personalized Knowledge-Based Inference**. Based on past charging records (step 1), we initially create a personalized knowledge-based inference model to infer personalized preference scores for unvisited ICSs using offline learning. This model captures the interaction between users and ICSs, as well as the relative information among ICSs, allowing for iterative learning (step 2) of the latent factors of EV users and ICSs to infer their charging preferences (step 3).
- **Online Candidate Arrangement Selection**. Upon receiving a charging request (step 4), we use an online candidate arrangement selection that treats the selection of charging arrangements as an online generalized assignment problem, with the goal of selecting profitable candidates (step 5) while taking into account future charging requests.
- **Interactive Arrangement Recommendation**. An interactive arrangement recommendation is also deployed to use the explore-exploit strategy to select the optimal charging arrangement for the EV user (step 6) and dynamically make recommendation decisions based on user feedback (step 7).

By learning the implicit preferences of users and selecting the most suitable charging arrangements, we can improve the WTA of users and balance the use of parking spots, ultimately leading to increased profits for all ICSs.

3.1 Personalized Knowledge-Based Inference

To optimize ICS operations, scheduling users' charging requests across various time slots and charging stations is vital. Our approach involves implementing an incentive strategy within a fixed budget to enhance the WTA of EV users. As expected, inferring users' initial charging preferences is crucial to making profitable decisions regarding the arrangement.

The main goal of our research is to discover the charging preferences for all ICSs, including those that have not been visited yet. This can be done by looking at the users' past charging records, which can give us an idea of their personal charging preferences. To achieve this, we propose a personalized knowledge-based inference approach that models two charging relationships as shown in Figure 3

(a.): (i) the relationships between EV users and ICSs, and (ii) the relationships among ICSs. This approach involves learning latent factor vectors of EV users and ICSs to infer the personalized preference ranking of all ICSs for each EV user.

3.1.1 Modeling Relationships between EV Users and ICSs. To infer users' charging preferences, we utilize the Bayesian personalized ranking (BPR) process [27] to estimate implicit charging preferences for all ICSs, including unvisited ones. Our goal is to provide each user v_i with a personalized total ranking $>_{v_i} \subset \mathcal{N}^2$ of all ICSs. Assume that $\mathbb{U}_{v_i}$ consists of triples of the form (v_i, n_j, n_k) with $n_j >_{v_i} n_k$ denoting that user v_i charges at ICS n_j more frequently than at ICS n_k. We define $\mathbb{U} = \bigcup_{v_i \in \mathcal{V}} \mathbb{U}_{v_i}$ as the collective set formed from the historical charging records of all EV users $\mathcal{V}$.

The objective of BPR in this context is to maximize the posterior probability, aiming to provide each EV user v_i with an accurate personalized ranking list and to obtain personalized preference scores for all ICSs $n \in \mathcal{N}$:

$$\mathcal{P}(\theta| >_{v_i}) \propto \mathcal{P}(>_{v_i} |\theta)\mathcal{P}(\theta), \tag{3}$$

where $>_{v_i}$ represents the latent charging preference structure for user v_i, and θ denotes the parameter vector of an arbitrary model (e.g., matrix factorization). The user-specific likelihood function $\mathcal{P}(>_{v_i} |\theta)$ can first be expressed as a product of individual probabilities, referring to the likelihood of user v_i's preference for each ICS pair. Then, this product is aggregated across all EV users in $\mathcal{V}$.

$$\prod_{v_i \in \mathcal{V}} \mathcal{P}(>_{v_i} |\theta) = \prod_{v_i, n_j, n_k \in \mathbb{U}} \mathcal{P}(n_j >_{v_i} n_k|\theta) := \prod_{v_i, n_j, n_k \in \mathbb{U}} \sigma(x_{ijk}(\theta)), \tag{4}$$

where $\sigma(x) := 1/(1 + e^{-x})$, and $\mathcal{P}(n_j >_{v_i} n_k|\theta)$ denotes the probability that user v_i is more likely to charge at ICS n_j than at ICS n_k (ranking n_j higher than n_k). In addition, $x_{ijk}(\theta)$ is a real-valued function of the model parameter vector θ that captures the special relationship between user v_i, ICSs n_j and n_k.

Based on the matrix factorization, the function $x_{ijk}(\theta)$ (abbreviated as x_{ijk}) can be expressed by $x_{ij} - x_{ik}$, and $x_{ij} := \mathbf{v}_i \cdot \mathbf{n}_j^{\mathrm{T}}$, where $\mathbf{v}_i, \mathbf{n}_j \in \mathbb{R}^m$ are the latent factor vectors of user v_i's preferences and ICS n_j, respectively. We assume that prior $\mathcal{P}(\theta) \sim \mathcal{N}(0, \lambda_\theta \mathbf{I})$ follows a normal distribution with zero mean and covariance matrix $\lambda_\theta \mathbf{I}$. Finally, the objective function of BPR is to minimize the negative log-likelihood, which can be derived as follows:

$$\begin{aligned} O_{uc} &= -\ln \mathcal{P}(>_{v_i} |\theta)\mathcal{P}(\theta) = \ln \prod_{v_i, n_j, n_k \in \mathbb{U}} \sigma(x_{ijk}(\theta))\mathcal{P}(\theta) = -\sum_{v_i, n_j, n_k \in \mathbb{U}} \left(\ln \sigma(x_{ijk}(\theta)) + \ln \mathcal{P}(\theta)\right) \\ &= \sum_{v_i, n_j, n_k \in \mathbb{U}} -\ln \sigma(\mathbf{v}_i \cdot \mathbf{n}_j^{\mathrm{T}} - \mathbf{v}_i \cdot \mathbf{n}_k^{\mathrm{T}}) + \lambda_i \|\mathbf{v}_i\|^2 + \lambda_j \left\|\mathbf{n}_j\right\|^2 + \lambda_k \|\mathbf{n}_k\|^2, \end{aligned} \tag{5}$$

where λ_i, λ_j and λ_k are regularization terms used to prevent overfitting.

3.1.2 Modeling Relationships among ICSs. In addition to modeling the relationships between EV users and ICSs, we also consider the relationships among ICSs to discover users' implicit charging preferences. For example, individuals who prefer shopping at supermarkets may also favor charging their electric vehicles at ICSs associated with supermarkets. Hence, we define *relative relationships* between ICSs based on the characteristics of integrated retail buildings.

Definition 6 (Relative Relations): Assuming that an ICS has m characteristics (in our scenario, three key characteristics of the ICS are considered, as outlined in Definition 1), we denote the set of relative relations as $L = \{l_1, l_2, ..., l_{2^m-1}\}$. Each relation $l_k \in L$ represents the equivalence of characteristics between ICSs. The relation type between two ICSs is determined by their shared characteristics. Therefore, the size of the relative relation set L is $2^m - 1$, excluding the case where two ICSs do not

Table 1. The comparison of Cosine similarity, Spearman correlation and Jaccard similarity of EV users' visiting frequency at ICSs with different characteristic equivalence.

	Geographic			Category		
Sets of ICS pairs	Cosine	Spearman	Jaccard	Cosine	Spearman	Jaccard
C	0.1824	0.1708	0.2051	0.1947	0.1460	0.2615
U	0.0107	-0.0195	0.0582	0.0158	-0.0185	0.0705

	Geographic & Category		
Sets of ICS pairs	Cosine	Spearman	Jaccard
C	0.2794	0.3107	0.3499
U	0.0172	-0.0232	0.0735

share any equivalent characteristics. Note that for the characteristic of geographic location, two ICSs are considered to have a relative relation indicating geographic equivalence if their distance is less than the average distance among all pairs of ICSs.

Based on the defined relative relations, we construct a specific knowledge graph called the *Relative Knowledge Graph*, which represents the relative information between ICSs.

Definition 7 (Relative Knowledge Graph): A relative knowledge graph (abbreviated as relative KG) is defined as $G = \{(n_i, l, n_j)|n_i, n_j \in \mathcal{N}, l \in L\}$, where $\mathcal{N}$ is the ICS set, and L is the relative relation set. Each triplet (n_i, l, n_j) states a fact that two ICSs n_i and n_j are with the relation type l. Note that the relations in G are symmetric, meaning that if (n_i, l, n_j) exists in G, then the triplet (n_j, l, n_i) also exists in G.

Analysis on the Relative KG. We examine the similarity of EV users' visiting frequencies between every two ICSs connected/unconnected in the proposed relative KG. We specifically explore geographic and category equivalence between two ICSs to investigate if these equivalences potentially correlate with EV users' charging choices. For category equivalence, let c_i and u_i denote the number of ICSs with specific relations and without specific relations with ICS $n_i \in \mathcal{N}$, respectively. We construct the following two sets for each ICS n_i with the same size $s = \min(c_i, u_i)$: (i) C_i includes randomly selected ICSs which have relations representing equivalent category with ICS n_i, forming the connected ICS pair $\mathbf{C} = \{(n_i, n_j)|n_j \in C_i, i = 1, 2, ..., \mathcal{N}\}$; (ii) U_i contains randomly selected ICSs that do not have relations representing equivalent category with n_i, forming unconnected ICS pair $\mathbf{U} = \{(n_i, n_j)|n_j \in U_i, i = 1, 2, ..., \mathcal{N}\}$. For geographic equivalence and the equivalence in both category and geographic, the sets $\mathbf{C}$ and $\mathbf{U}$ are constructed similarly.

We represent EV users' visiting frequencies as vectors $\mathbf{f}_i \in \mathbb{R}^{|\mathcal{V}|}$ and $\mathbf{f}_j \in \mathbb{R}^{|\mathcal{V}|}$ for each ICS pair (n_i, n_j) in $\mathbf{C}$ and $\mathbf{U}$. Here, the k^{th} element in vector $\mathbf{f}_i$ indicates the visiting frequency of EV user $v_k \in \mathcal{V}$ at ICS n_i. We then estimate the similarity between vectors $\mathbf{f}_i$ and $\mathbf{f}_j$ for each ICS pair in sets $\mathbf{C}$ and $\mathbf{U}$, as shown in Table 1. According to Table 1, users' visiting frequencies for ICS pairs in the connected set $\mathbf{C}$ exhibit significantly higher similarity compared to those in the unconnected set $\mathbf{U}$. Furthermore, ICS pairs in $\mathbf{C}$ that share more characteristics (Geographic & Category) demonstrate even stronger similarity and correlation. While the similarity scores for the connected set $\mathbf{C}$ are modest, this analysis underscores the potential of a few but general characteristics of ICSs to enhance charging recommendations. Note that although our analysis focuses on certain characteristics, the structure of the relative KG facilitates the easy incorporation of additional characteristics.

Consequently, we propose a novel knowledge graph embedding method that incorporates both the characteristics of ICSs and the similarity of their visiting EV users. By leveraging the idea of message passing [16, 41], we update the latent factor of an ICS by aggregating information from its neighboring ICSs in the relative KG. Denoting the latent factor of ICS n_i at the previous stage as $\mathbf{n}_i$, and considering the set of direct neighbors (1-hop neighbors) of n_i in the relative KG G as $N(n_i)$, we

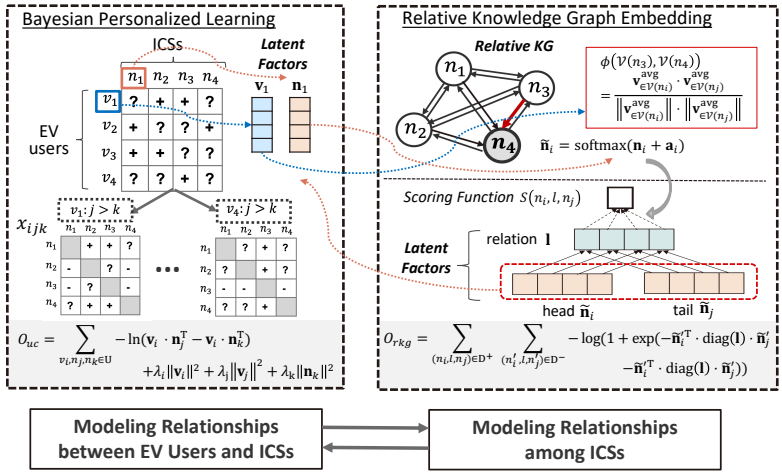

Fig. 4. The process of personalized knowledge-based inference.

define the updated latent factor $\tilde{\mathbf{n}}_i$ for n_i as follows:

$$\tilde{\mathbf{n}}_i = \mathrm{softmax}\big(\mathbf{n}_i + \mathbf{a}_i\big) \quad \text{with} \quad \mathbf{a}_i = \sum_{n_j \in N(n_i)} \phi\big(\mathcal{V}(n_i), \mathcal{V}(n_j)\big) \cdot \mathbf{n}_j, \tag{6}$$

where $\mathbf{a}_i$ is the aggregated latent factor from the neighbor set $N(n_i)$. The sets $\mathcal{V}(n_i)$ and $\mathcal{V}(n_j)$ denote users who have charged at ICSs n_i and n_j, respectively. The function $\phi(\cdot,\cdot)$ is used to estimate the similarity between two user sets. To calculate the similarity, we consider the current average latent factors $\bar{\mathbf{v}}_{\in\mathcal{V}(n_i)}$ of users belonging to $\mathcal{V}(n_i)$. The similarity function $\phi(\cdot,\cdot)$ is defined as follows:

$$\phi\big(\mathcal{V}(n_i), \mathcal{V}(n_j)\big) = \frac{\bar{\mathbf{v}}_{\in\mathcal{V}(n_i)} \cdot \bar{\mathbf{v}}_{\in\mathcal{V}(n_j)}}{\big\|\bar{\mathbf{v}}_{\in\mathcal{V}(n_i)}\big\| \times \big\|\bar{\mathbf{v}}_{\in\mathcal{V}(n_j)}\big\|}. \tag{7}$$

Therefore, according to Eqs.6 and 7, the energy function of each triplet (n_i, l, n_j) is designed based on DistMult[43] model, and it can be formulated as follows:

$$S(n_i, l, n_j) = \tilde{\mathbf{n}}_i^{\mathrm{T}} \cdot \mathrm{diag}(\mathbf{l}) \cdot \tilde{\mathbf{n}}_j, \tag{8}$$

where $\mathbf{l}$ is the latent factor of relation l.

Finally, we design the objective function for embedding the relative KG using the pairwise logistic loss, which is formulated as follows:

$$\begin{aligned} O_{rkg} &= \sum_{(n_i,l,n_j)\in\mathbb{D}^+} \sum_{(n_i',l,n_j')\in\mathbb{D}^-} -\log\Big(1 + \exp\big(\mathcal{S}(n_i,l,n_j) - \mathcal{S}(n_i',l,n_j')\big)\Big) \\ &= \sum_{(n_i,l,n_j)\in\mathbb{D}^+} \sum_{(n_i',l,n_j')\in\mathbb{D}^-} -\log\Big(1 + \exp\big(\tilde{\mathbf{n}}_i^{\mathrm{T}} \cdot \mathrm{diag}(\mathbf{l}) \cdot \tilde{\mathbf{n}}_j - \tilde{\mathbf{n}}'^{\mathrm{T}}_i \cdot \mathrm{diag}(\mathbf{l}) \cdot \tilde{\mathbf{n}}_j'\big)\Big), \end{aligned} \tag{9}$$

where $\mathbb{D}^+$ and $\mathbb{D}^-$ are the positive and the negative triplet sets, respectively. The objective is to minimize the marginal difference between the negative and positive scores, using a smoother linear slope compared to hinge loss.

3.1.3 Model Training and Optimization. In our personalized knowledge-based inference, the latent factors of EV users and ICSs are updated simultaneously during each training epoch. As shown in Figure 4, at the t-th epoch, the latent factor vectors $\mathbf{v}_i^t$ for each user and $\mathbf{n}_j^t$ for each ICS are obtained by modeling the relationships between EV users and ICSs. These obtained ICS vectors $\mathbf{n}_j^t$

serve as input for modeling the relationships among ICSs, while the user vectors $\mathbf{v}_i^t$ are used to update the ICS vectors by aggregating information from neighboring ICSs. After optimizing the pairwise logistic loss of the relative KG embedding, the updated ICS vectors $\mathbf{n}_j^{t+1}$ are output and used as the initial vectors for the next training epoch. Therefore, the final objective function of personalized knowledge-based inference can be formulated as follows:

$$\begin{aligned}
&\min_{\boldsymbol{\mathcal{V}},\boldsymbol{\mathcal{N}}}(O_{uc}) + (O_{rkg}) \\
&= \sum_{v_i,n_j,n_k\in\mathbb{U}} -\ln(\mathbf{v}_i\cdot\mathbf{n}_j - \mathbf{v}_i\cdot\mathbf{n}_k) + \lambda_i\left\|\mathbf{v}_i\right\|^2 + \lambda_j\left\|\mathbf{n}_j\right\|^2 + \lambda_k\left\|\mathbf{n}_k\right\|^2 \\
&- \sum_{(n_i,l,n_j)\in\mathbb{D}^+}\ \sum_{(n_i',l,n_j')\in\mathbb{D}^-} \log\Big(1+\exp\big(\tilde{\mathbf{n}}_i\cdot\mathrm{diag}(\mathbf{l})\cdot\tilde{\mathbf{n}}_j - \tilde{\mathbf{n}}_i'\cdot\mathrm{diag}(\mathbf{l})\cdot\tilde{\mathbf{n}}_j'\big)\Big).
\end{aligned} \tag{10}$$

The objective function aims to learn the latent factors of all EV users and ICSs ($\boldsymbol{\mathcal{V}}$ and $\boldsymbol{\mathcal{N}}$) to infer the personalized preference ranking of ICSs for each EV user. Finally, by learning the optimal latent factor vectors of EV users and ICSs, a user's implicit charging preferences for all ICSs can be calculated. For the EV user v, the personalized preference score for an ICS n is denoted as $x_{v,n} = \mathbf{v}_i\cdot\mathbf{n}_j^{\mathrm{T}}$. Let $\mathcal{N}_\tau^v$ be the set of ICSs where user v charged in time slot τ in the historical charging records, the personalized preference score $p_{n,\tau}^v$ of user v to charge at ICS n in time slot τ is formulated as follows:

$$p_{n,\tau}^v = \frac{\sum_{n_q\in\mathcal{N}_\tau^v}\big(sim(\mathbf{n},\mathbf{n}_q)\cdot c_{q,\tau}\big)}{Z}\cdot x_{v,n}, \tag{11}$$

where $c_{q,\tau}$ is the count that v charges at time slot τ in the historical charging records. The function $sim(\cdot,\cdot)$ is a cosine similarity function that estimates the similarity between two latent factors, and Z is a normalization term.

3.2 Online Candidate Arrangement Selection

After obtaining inferred personalized preference scores of EV users, we use the incentive strategy with a fixed budget to enhance the WTA of users as shown in Figure 3(b.). Considering the uncertainty of future charging information, we need to determine the most profitable charging arrangement for the current charging request to generate profits for all ICSs.

In the previous work *POSIT* [38], a charging scheduling algorithm based on the online knapsack problem is developed [47]. However, in this paper, we extend to the scenario of multiple ICSs with different incentive budgets. The recommendation of different charging time slots and ICSs to EV users does not always yield the same profits, resembling the generalized assignment problem [25]. The generalized assignment problem (GAP) is that knapsacks of different capacities are given, and the size and the profit of an item depend on the knapsack to which it is assigned. Therefore, without knowing future charging requests in our scenario, we translate our charging problem into an online generalized assignment problem (OGAP), where charging requests arrive sequentially, and we recommend when and where to charge based on the current information. In our scenario of online recommendation, the incentive budgets of multiple ICSs represent multiple knapsacks with different capacities, and each possible charging arrangement corresponds to an item to decide whether to recommend it or not.

To determine profitable charging arrangements for ICSs, we define a *benefit score* for each arrangement and apply an online threshold-based algorithm to select candidates. We consider the benefit score and the provided incentive as the item value and weight in our OGAP problem, respectively. Our objective is to find a set of candidate charging arrangements where each arrangement has a value-to-weight ratio higher than a specified threshold.

3.2.1 Benefit Score Estimations. As mentioned in Sec. 1, unbalanced utilization of ICSs may lead to higher penalty costs for popular ICSs and reduced profits for less popular ones with numerous available charging positions. Moreover, focusing solely on a target user's acceptance of a recommended arrangement, without considering the willingness of other users, may inadvertently create new demand peaks at different time slots. This can lead to increased penalty costs. To tackle these issues, we estimate a *benefit score* for each charging arrangement in a simple but effective way, taking into account two factors: the *user willingness factor* and the *utilization balance factor*. These two factors help us to determine the profitability of a charging arrangement.

User Willingness Factor: Considering the challenge highlighted in previous studies [13, 20], which indicate that addressing original demand peaks may inadvertently introduce new ones (rebound peaks), we define a charging arrangement as profitable if it aligns with high willingness from target user v and low willingness from other users. Therefore, we introduce the *user willingness factor*, which considers both individual and group charging willingness for each arrangement.

Let $M^v = (n, \tau, \vartheta)$ denote a recommended charging arrangement for user v, where n, τ and ϑ represent the recommended ICS, charging time slot, and the amount of incentive provided to user v, respectively. The user willingness factor $\mathcal{F}_w(M^v)$ for user v with the recommended arrangement M^v is designed as follows:

$$\mathcal{F}_w(M^v) = \alpha \cdot P_{indiv}(M^v) + (1-\alpha)(1 - P_{group}(M^v)), \tag{12}$$

where $P_{indiv}(M^v)$ and $P_{group}(M^v)$ represent the WTA (willingness to accept) of the individual and the group for the arrangement M^v, respectively. The constant value α is used to control the effects of these two kinds of willingness. Both WTA values range from 0 to 1.

The individual WTA $P_{indiv}(M^v)$ to the arrangement $M^v = (n, \tau, \vartheta)$ represents the WTA of user v to charge at ICS n at time slot τ after receiving the incentives ϑ. In Sec. 3.1, we infer the personalized preference score $p^v_{n,\tau}$ for each user v, which represents the user's implicit WTA (the blue points shown in Figure 3 (b.)). However, the WTA may change after providing incentives. According to the survey [40], higher monetary incentives can increase users' willingness to adjust their charging behaviors, but as the incentive amount grows, the rate of increase in user participation diminishes, indicating reduced effectiveness in boosting willingness. Consequently, inspired by earlier research [10, 34] that applied sigmoidal-like functions to depict shifts in users' willingness, preference, or satisfaction, we employ a sigmoidal-like utility function to represent the variation in users' WTA (the red points shown in Figure 3 (b.)) as incentives increase. We hypothesize that the WTA will initially rise quickly with the addition of incentives, and then the rate of increase will gradually slow. As such, the individual WTA $P_{indiv}(M^v)$ (regarded as changed WTA of user v) is defined as follows:

$$P_{indiv}(M^v) = \sigma\left(\ln\left(\frac{p^v_{n,\tau}}{1 - p^v_{n,\tau}}\right) + \beta \cdot \vartheta\right), \tag{13}$$

where $\sigma(x) = 1/(1 + e^{-x})$ is a sigmoid function. β is a fixed constant value.

On the other hand, the group WTA $P_{group}(M^v)$ defines the average WTA of other users, excluding user v, towards the arrangement M^v. It is calculated as the average charging willingness of all users, given by the following expression:

$$P_{group}(M^v) = \frac{\sum_{v \in \mathcal{V} - \{v\}} p^v_{n,\tau}}{|\mathcal{V}|}. \tag{14}$$

Based on the individual WTA $P_{indiv}(M^v)$ and the group WTA $P_{group}(M^v)$, the *user willingness factor* $\mathcal{F}_w(M^v)$ for user v with the recommended arrangement M^v can be estimated using Equation 12.

Utilization Balance Factor: We also introduce the *utilization balance factor* to determine the profitability of a charging arrangement. We consider that a charging arrangement is beneficial if it can help balance the utilization of charging positions across all ICSs at the same time slot. Let a recommended charging arrangement for user v be $M^v = (n, \tau, \vartheta)$, and let $u_{n,\tau}$ be the utilization value of parking positions at ICS n at time slot τ, which is estimated as the ratio of *the number of occupied parking positions* to *the value of ideal available capacity*. Therefore, the *utilization balance factor* of the arrangement M^v is defined as follows:

$$\mathcal{F}_b(M^v) = \frac{u_\tau^{\text{avg}} - u_\tau^n}{u_\tau^{\max}}, \tag{15}$$

where u_τ^{avg} and $u_\tau^{\max}$ are the average and maximum values of utilization among all ICSs, respectively.

According to the designed *user willingness factor* $\mathcal{F}_w(M^v)$ and the *utilization balance factor* $\mathcal{F}_b(M^v)$ for the recommended charging arrangement M^v, the benefit score of M^v can be estimated. Assuming that an EV user v sends a charging request with a requested charging duration of $h \in \mathbb{Z}^+$ (Def. 3), the benefit score ε^{M^v} is formulated as follows:

$$\varepsilon^{M^v} = \begin{cases} 0 & \text{, if } \min\{\tilde{l}_\tau^n, \tilde{l}_{\tau+1}^n, ..., \tilde{l}_{\tau+h-1}^n\} = 0 \\ \left(\hat{n}\left(\mathcal{F}_w(M^v)\right) + \xi\right) \cdot \left(\hat{n}\left(\mathcal{F}_b(M^v)\right) + \xi\right) & \text{, otherwise} \end{cases}, \tag{16}$$

where $\tilde{l}_\tau^n$ represents the inferred number of remaining parking positions, estimated by subtracting the number of occupied parking positions from the ideal available capacity l_τ^n (Def. 4). The function $\hat{n}(\cdot)$ is used to normalize the factor value to range from 0 to 1. Additionally, $\xi > 0$ is an extremely small value introduced to prevent the benefit score ε^{M^v} from becoming 0 when there still exist available parking positions. With this design, a higher value of the *user willingness factor* or the *utilization balance factor* indicates a more profitable charging arrangement.

3.2.2 Online Threshold-Based Estimation. Based on the benefit score ε^{M^v}, we can identify candidate arrangements that are profitable for ICSs and also possess a certain level of acceptance from EV users. To determine whether a charging arrangement $M^v = (n, \tau, \vartheta)$ is profitable, the value-to-weight ratio for M^v is estimated. Consequently, the set of candidate arrangements $\mathbf{M}^v$ for the charging request sent by EV user v should satisfy the following condition:

$$\mathbf{M}^v = \{M^v | \frac{\varepsilon^{M^v}}{\vartheta} > \varphi^n\}, \tag{17}$$

in which φ^n is a threshold value of the recommended ICS n, and ϑ is the provided incentive. In our OGAP charging problem, the benefit score ε^{M^v} and the provided incentives ϑ are regarded as the value and the weight of the arrangement M^v, respectively. If the value-to-weight ratio of M^v exceeds the threshold, M^v is considered a candidate for the profitable charging arrangement for ICSs and EV user v.

3.3 Interactive Arrangement Recommendation

To determine which charging arrangement from the candidate set $\mathbf{M}^v$ should be recommended to EV users, an interactive planning process is developed in this paper based on user feedback. This strategy aims to understand the overall acceptance of EV users to various charging arrangements. Specifically, reinforcement learning technology [19] is employed to facilitate the selection of the most suitable action through user feedback. We model our interactive arrangement scheduling as a Markov Decision Process (MDP) problem.

3.3.1 MDP Formulation. Assuming that at iteration t, the set of candidate arrangements (Eq.17) is denoted as $\mathbf{M}_t^v$, we formulate an MDP problem. This encompasses a sequence of states, actions, and rewards to model the interaction of recommendation with all EV users, defined as follows:

States $\mathcal{S}$: A state $s_t \in \mathcal{S}$ captures the dynamics between the charging arrangement $M_t^v \in \mathbf{M}_t^v$ recommended to the current EV user v at iteration t. This includes (i) the visiting ratio of user v to the recommended ICS based on the historical charging records, (ii) the time difference between the recommended charging time slot and user v's preferred charging times in the past, (iii) the provided incentives in M_t^v, and (iv) the division of the benefit score $\varepsilon^{M_t^v}$ into ranges with a fixed width, determining the range of $\varepsilon^{M_t^v}$. Note that each iteration corresponds to a recommendation for an EV user's charging request.

Actions $\mathcal{A}$: An action $a_t \in \mathcal{A}$ is to recommend a charging arrangement to an EV user at each iteration t.

Rewards $\mathcal{R}$: A reward $r_t \in \mathcal{R}$ is given based on EV users' feedback. To capture the overall acceptance of specific charging arrangements by EV users, the reward value is designed in a straightforward manner: If user v accepts the recommended arrangement M_t^v (corresponding to state s_t), the reward $r(s_t, a_t) = 1$; otherwise, $r(s_t, a_t) = 0$ as default.

3.3.2 Q-learning for Charging Recommendation. Q-learning aims to select an action a_t that maximizes the Q-value $Q^*(s_t, a_t)$ for each state s_t. In each iteration t, the optimal Q-value, considering the optimal policy with action a_t for the current state s_t, is defined as the sum of the accumulated reward and the expected reward when transitioning from the current state s_t to the next state s_{t+1}:

$$Q^*(s_t, a_t) = \mathbb{E}_{s_{t+1} \sim T(.|s_t, a_t)}[r_t + \gamma \max_{a_{t+1}} Q^*(s_{t+1}, a_{t+1}) | s_t, a_t], \tag{18}$$

where $0 < \gamma \leq 1$ is a discount factor, and its Bellman optimality operator Ψ_B is thus defined as follows:

$$\Phi_{\mathcal{B}} q(s_t, a_t) = r_t(s, a) + \gamma \mathbb{E}[\max_{a_{t+1}} Q^*(s_{t+1}, a_{t+1}) | s_t, a_t]. \tag{19}$$

The Bellman operator helps prove the convergence of reinforcement learning to a unique fixed point. In our paper, we further consider the charging arrangement recommendation in Q-learning to identify the most profitable charging arrangement. According to the *Nearest Neighbor Q-Learning* (NNQL) algorithm [31], the Q value of a specific (s, a) is influenced by both the rewards it gains and the Q values of nearby observations. Similarly, in our scenario, different incentives with the same charging time slots and ICSs are expected to be comparable, meaning their Q-values shall affect each other.

Consequently, we identify a subset $\tilde{\mathbf{M}}_t \subseteq \mathbf{M}_t^v$ of charging arrangements, including candidates similar to the arrangement $M_t^v = (n_t, \tau_t, \vartheta_t)$ recommended to user v at iteration t (corresponding to state s_t). An arrangement $(n', \tau', \vartheta') \in \tilde{\mathbf{M}}_t$ must satisfy $n_t = n'$ and $\tau_t = \tau'$, and $q(s', a_t) \neq 0$, where $s' \in \mathcal{S}$ represents the state corresponding to arrangement (n', τ', ϑ') for user v. Given the estimated Q-values $\{q(s_t, a_t) | s_t \in \mathcal{S}, a_t \in \mathcal{A}\}$, the operator $\Phi_{\mathcal{I}}$ for our interactive arrangement recommendation can be expressed as follows:

$$\Phi_{\mathcal{I}} q(s_t, a_t) = \sum_{(n', \tau', \vartheta') \in \tilde{\mathbf{M}}_t} \Big((1 - \frac{|\vartheta_t - \vartheta'|}{\sum_{(\hat{n}, \hat{\tau}, \hat{\vartheta}) \in \tilde{\mathbf{M}}_t} |\vartheta_t - \hat{\vartheta}|}) \cdot q(s', a_t) \Big). \tag{20}$$

According to Eq.19 and Eq.20, the joint operator $\Phi_{\mathcal{BI}}$ can be expressed as follows:

$$\Phi_{\mathcal{BI}} q(s_t, a_t) \triangleq (\Phi_{\mathcal{B}} \Phi_{\mathcal{I}} q)(s_t, a_t) = r_t(s, a) + \gamma \mathbb{E}[\max_{a_{t+1}} \Phi_{\mathcal{I}} q(s_{t+1}, a_{t+1}) | s_t, a_t], \tag{21}$$

which is the operator that our optimization aims to approximate. The Q-value of the interactive arrangement recommendation $\tilde{Q}_t(s_t, a_t)$ for a state-action pair (s_t, a_t) at each iteration t is updated based on the joint operator $\Phi_{\mathcal{BI}}$ as follows:

$$\tilde{Q}_t(s_t, a_t) = (\Phi_{\mathcal{BI}} q)(s_t, a_t) = (1-\eta)(\Phi_{\mathcal{BI}} q)(s_t, a_t) + \eta(r_t + \gamma \max_{a_{t+1}} \Phi_I q(s_{t+1}, a_{t+1})), \quad (22)$$

where $0 \leq \eta \leq 1$ is the learning rate. We update $\tilde{Q}_{t+1}(s_t, a_t)$ using the following rule:

$$\tilde{Q}_{t+1}(s_t, a_t) = \tilde{Q}_t(s_t, a_t) + \eta(r_t + \gamma \max_{a_{t+1}} \tilde{Q}(s_{t+1}, a_{t+1}) - \tilde{Q}_t(s_t, a_t)). \quad (23)$$

After updating the Q-values at each iteration, we utilize the ϵ-greedy method to balance exploration and exploitation. The charging arrangement selection policy for each iteration t is described as follows:

$$a^* = \begin{cases} random(\mathcal{A}), & if \ \xi \leq \epsilon. \\ \arg\max_{a_t \in \mathcal{A}} \tilde{Q}^*(s_t, a_t), & otherwise. \end{cases} \quad (24)$$

Finally, the optimal policy for actions that maximize rewards can be discovered. For an EV user v, we can estimate which charging arrangement in the candidate set $\mathbf{M}_t^v$ is the most profitable, aiming to enhance the WTA of the user and increase profits for all ICSs.

4 EXPERIMENTS

4.1 Dataset and Experimental Setup

4.1.1 ***Datasets.*** We utilize various real-world datasets for this study. For the charging stations and EV charging information, we use the EV charging dataset from Drive Dundee Electric [9], which includes EV charging details of chargers in Dundee, Scotland in 2018. The dataset provides information such as user ID, charge point ID, geographic coordinates of charge points, plug-in and unplug times, and energy delivered during the session. From this dataset, we select 20 charge points as our ICSs (Integrated Charging Stations) and randomly assign different numbers of chargers (ranging from 2 to 10) to each ICS. Regarding the information of integrated retail buildings associated with ICSs, we identify the closest store to each selected ICS using Google Maps. The selected store serves as the integrated retail building for an ICS.

For electricity consumption data of retail buildings and PV generation data, we utilize the EnerNOC dataset [26] and the UMass Smart* SunDance dataset [6], respectively. From these datasets, we select data from 20 commercial sites and solar sites as the electricity consumption and PV generation data for our 20 integrated retail buildings. We merge these datasets and select six months of data as the training set for our electricity forecasting model (the LSTM model in Def. 4). To ensure consistency across datasets from different years, we selected data from the same months. Specifically, we use data from January 7 to July 7, 2018, from the Drive Dundee Electric dataset, January 7 to July 7, 2012, from the EnerNOC dataset, and January 7 to July 7, 2015, from the UMass Smart* SunDance dataset for training. The subsequent seven days following these dates are used as the testing dataset to evaluate the performance of our *POSKID* framework. Note that all the data used in this study are standardized and consolidated into hourly data.

4.1.2 ***Implementation Details.*** For implementing the LSTM model to predict PV generation and energy consumption for the retail building associated with an ICS (as mentioned in Def. 4), we employ the training dataset (mentioned in Sec. 4.1.1) and apply a sliding window approach with a span of five days, using the first four days for training and the subsequent day for testing. During the testing phase of *POSKID*, the pre-trained LSTM predicts PV generation and energy consumption for each ICS hourly, aiding in inferring the ideal available capacity of each ICS. To address inaccuracies in LSTM predictions, if the actual total electricity consumption (minus actual PV generation) exceeds

the contracted capacity at any hour on the previous day, we adjust the inferred ideal available capacity by reducing it by one for that hour on the current day.

4.1.3 ***Electricity Price Setting.*** For estimating electricity costs, we adopt the price settings in [21], which uses Time-of-Use (TOU) rates based on the Southern California Edison TOU EV-4 tariff schedule as shown in Table 2. We choose TOU for its balance between the simplicity of single-price systems over extended periods and the complexity of real-time pricing systems common in wholesale markets [17], underscoring the practicability of our method for real-world applications.

The contracted electrical capacity of each Integrated Charging Station (ICS) is set to the average value of the top 10% highest electricity consumption among the integrated retail buildings in the training dataset. To calculate the electricity cost for an ICS n, both the capacity rate and the energy rate are taken into account. In particular, electrical operating cost comprises the basic charge, the penalty charge, and the energy charge. Assuming that the contracted electrical capacity for ICS n is 30 kW, we outline the calculation of these three charges as follows.

- **Basic Charge**: A fixed basic charge is applied if the peak electricity demand of ICS n stays within this limit ($\leq$ 30 kW). The basic charge is based on the capacity rate (15.51 USD/kW) listed in Table 2, calculated as 30 kW * 15.51 USD/kW = 465.3 USD.
- **Penalty Charge**: According to [28], exceeding the contracted capacity triggers an additional penalty charge at an *uncontracted rate*, which is often three times higher than the capacity rate or more. In our scenario, the uncontracted rate is set at *twice the capacity rate*. Thus, if the peak demand of ICS n is 50 kW, which surpasses the contracted capacity (> 30 kW), the penalty charge would be (50-30) * 2 * 15.51 USD/kW = 620.4 USD, in addition to the basic charge of 465.3 USD.
- **Energy Charge**: The energy charge is determined by the amount of energy consumed (in kilowatt-hours, or kWh) during peak, semi-peak, and off-peak periods, with each period having a distinct rate as outlined in Table 2.

4.1.4 ***User Simulated Behaviors.*** To simulate whether an EV user will accept the recommended charging arrangement or not, we assume that the acceptance probability of users follows a sigmoidal-like function [10, 34]. The acceptance probability of EV user v for a recommended charging arrangement $M^v = (n, \tau, \vartheta)$ is defined as $P_{accept}(M^v) = \sigma\big(\ln\big((1-d)/d\big) + \kappa \cdot \vartheta\big)$, which is similar to the modeling of increasing users WTA in Eq.13, while we adjust the value κ to $\{0.15, 0.20, 0.25\}$ to simulate the different degree of user acceptance according to the provided incentives.

The term d represents the discrepancy between the recommendation $M^v = (n, \tau, \vartheta)$ and the charging behavior of user v. We estimate discrepancy d based on the *historical behavior* and the *future behavior* of user v, leading to the development of two simulation strategies $\mathrm{S}_{\mathrm{history}}$ and $\mathrm{S}_{\mathrm{future}}$ as follows.

- **Simulation Strategy $\mathbf{S_{history}}$**: The discrepancy d is estimated by averaging three normalized factors from user v's *historical charging records*, namely, user v's charging records in the training dataset. We consider user v's most visited ICS as n_v^{hist} and their most frequent charging time slot as τ_v^{hist}. The factors include: (i) the infrequency ratio of user v visiting ICSs of the same category as the recommended ICS n, (ii) the time difference between the recommended time slot τ and τ_v^{hist}, and (iii) the distance from n to n_v^{hist}.
- **Simulation Strategy $\mathbf{S_{future}}$**: This strategy, while also estimating d by averaging three normalized factors, diverges by focusing on user v's *future charging behavior*—specifically, user v's original charging record in the testing dataset. With user v's original charging ICS and time slot denoted as n_v^{futu} and τ_v^{futu}, respectively, the factors include: (i) the category equivalence between n and n_v^{futu} (1 for equivalence, 0 otherwise), (ii) the time difference between τ and τ_v^{futu}, and (iii) the distance between n and n_v^{futu}.

Table 2. SCE EV TOU-4 rate schedule for EV charging in summer (unit price: USD).

Classification			Charge (USD)	
			Weekdays	Weekend
Capacity Rate	per kW		$ 15.51 /kW / month	
Energy Rate	Peak Time	12:00 - 18:00	$0.267 / kWh	$0.056 / kWh
	Mid-Peak Time	08:00 - 12:00 18:00 - 23:00	$0.092 / kWh	$0.056 / kWh
	Off-Peak Time	23:00 - 08:00	$0.056 / kWh	$0.056 / kWh

Therefore, a lower value of the discrepancy d or a higher incentive ϑ increases the likelihood of user v accepting the charging recommendation.

4.1.5 ***Baseline Methods.*** We compare *POSKID* with several baselines, categorized into three main groups: (i) traditional scheduling-based, (ii) KP-Based (knapsack problem-based), and (iii) incentive-based methods. All methods are designed for online charging scheduling in our scenario. For each charging request from EV user v, the first two types of methods provide the charging arrangement $M^v = (n, \tau)$, including the recommended ICS n and the time slot τ. The last type of method provides the charging arrangement $M^v = (n, \tau, \vartheta)$, including the recommended ICS n, the time slot τ, and the provided incentives ϑ.

- Traditional Scheduling-Based: **S-RR** recommends ICSs in the cyclical order, with the recommended charging time slot being the most frequently used one in user v's historical record. **ST-RR** recommends both ICSs and time slots in cyclical order. **Remain-RR** is similar to ST-RR but sorts all (n, τ) pairs in descending order based on the number of remaining parking positions at ICS n during the time slot τ in the past. **LLF-RR** recommends ICSs and time slots as similar to S-RR, but assigns higher priority to EV users with longer charging needs, allowing them to be recommended charging arrangements first.
- KP-Based: **FOCS** [2] and **SCOMMIT** [1] are designed based on the fractional knapsack problem, where charging requests with higher unit values are scheduled first. In our experiments, the unit value of a request is defined as (*the historical frequency of v charging at the recommended time slot*) / (*charging time duration*). ICSs are recommended in cyclical order, and time slots are recommended starting from user v's most preferred time slot.
- Incentive-Based: To verify the effectiveness of the benefit score (Eq. 16), we design **RI** and **RI-Q** as simplified versions of *POSKID*, randomly recommending different values of incentives to EV users. While RI-Q applies Q-learning techniques, RI simply recommends the charging arrangement with the highest benefit score. For the incentive-based methods, we also adjust the value of κ mentioned in Sec. 4.1.4 to $\{0.15, 0.20, 0.25\}$ to control users' enhanced acceptance probability when receiving incentives.

In addition to aforementioned methods, we also show the results of **Uncoordinated** to represent the performance of the uncoordinated scenario. Note that the evaluation of all methods adheres to the defined simulation strategies S_{history} and S_{future} (see Sec. 4.1.4) to simulate user acceptance behaviors.

4.1.6 ***Evaluation Settings.*** We design several evaluation metrics to evaluate the utilization balancing of parking positions, the operating costs of ICSs, and user satisfaction with the recommended charging arrangements.

- Operating Cost: the **Energy Charge** and the **Penalty Charge** are electricity charges defined as Sec. 4.1.3. **Incentive Cost** represents the amount of money given to EV users as incentives, applicable only to incentive-based methods. We allocate 400 charging coupons per day for all ICSs as the incentive budget. Since L2 chargers cost between USD 0.20-0.30 per kWh [36], we set the face

value of each coupon (incentive) at USD 0.30, providing a discount of 100% off the charging cost per kWh. **Total Cost** is the sum of the basic charge, the energy charge, the penalty charge, and the incentive cost. Note that the statistic for the basic charge is not provided, as it remains the same across all methods.

- User Dissatisfaction: We evaluate several metrics based on the user's total charging records, encompassing both the training and testing sets. The **Infrequency Ratio** is calculated as $1 - \frac{N_{visit}}{N_{total}}$, where N_{visit} denotes the number of times a user visits recommended ICS categories, and N_{total} represents the number of the user's total charging records. **Moving Distance** represents the distance between the recommended ICS and the user's most frequently visited ICS. **Time Difference** is the difference between the recommended time slot and the user's most frequently charged time slot. Finally, the **Dissatisfaction Score** is calculated as the average of normalized values from the evaluations mentioned above. Lower scores in category infrequency ratio, moving distance, or charging time difference lead to a reduced dissatisfaction score, signifying higher user satisfaction with the recommended ICS and charging time slot. These evaluations are averaged over all recommended charging arrangements.
- **Penalty-Plus-Dissatisfaction Score**: This score is used to evaluate the effectiveness of a method in managing both operating costs and user dissatisfaction. Since penalty charges significantly contribute to variations in operating costs across different methods, we design the Penalty-Plus-Dissatisfaction Score as a weighted sum of the normalized penalty charge and the dissatisfaction score, as illustrated below:

$$\omega \cdot \frac{M_{\text{penalty}}}{\max_{\text{penalty}}} + (1 - \omega) \cdot M_{\text{dissatis}}, \tag{25}$$

where M_{penalty} and M_{dissatis} represent the penalty charge and dissatisfaction score of a method M, repsecitvely. $\max_{\text{penalty}}$ denotes the maximum penalty charge among all methods, which is assigned to the penalty charge of "Uncoordinated" method. The value of ω is set to 0.5. A lower score signifies a method's superior capability in managing both operating costs and user dissatisfaction effectively.

Note that we satisfy all EVs' charging requests in our scenario, so the total charging revenues are the same in different scheduling methods.

4.2 Performance Comparison Results

We first compare *POSKID* with the aforementioned baselines. The comparison of operating cost and user dissatisfaction with two simulation strategies S_{history} and S_{future} are summarized in Table 3 and Table 4, respectively. These tables reveal the average performance of an ICS on all testing days. As demonstrated in Table 3 and Table 4, while *POSKID* may not secure the lowest dissatisfaction score, it achieves the lowest total cost and the minimal penalty-plus-dissatisfaction score under both simulation strategies S_{history} and S_{future}. This suggests that *POSKID* effectively minimizes total costs while maintaining user satisfaction, thus proving its practicability. In the following, we will discuss the detailed comparison with the baselines:

- In the operating cost comparison shown in Tables 3 and 4, energy charges across all methods are similar. However, *POSKID* significantly reduces penalty charges compared to other baselines, leading to the lowest total costs in both tables for $\kappa = 0.25$ and $\kappa = 0.15$, respectively. Notably, *POSKID* saves over USD 360 in seven testing days compared to the uncoordinated scenario across all κ settings. This highlights the ability of *POSKID* to benefit all ICSs, even with a minimal increase in users' acceptance probability ($\kappa = 0.15$) due to incentives.
- The uncoordinated scenario, which allows users to follow their original charging behaviors without any scheduling strategy, achieves the lowest dissatisfaction score. SCOMMIT and LLF-RR achieve

Table 3. Performance comparison with simulation strategy $S_{history}$. For the evaluation of "Total Cost" and "Dissatisfaction Score", the best and second-best results are highlighted in **bold** and marked with an asterisk (*), respectively. Cells highlighted in gray indicate results that rank in the lowest 40% for either total scores or dissatisfaction scores, excluding the scenario of "Uncoordinated".

Methods	Operating Cost				User Dissatisfaction				Overall
	Energy Charge (USD) (↓)	Penalty Charge (USD) (↓)	Incentive Cost (USD) (↓)	**Total Cost (USD) (↓)**	Infrequency Ratio (↓)	Moving Distance (km) (↓)	Time Difference (hr) (↓)	**Dissatisfaction Score (↓)**	**Penalty-Plus-Dissatisfaction Score (↓)**
Uncoordinated	3767.1	914.5	0	8606.5	0.212	0.650	0.271	0.101	0.550
S-RR	3765.0	902.6	0	8592.5	0.663	3.893	0.714	0.375	0.681
ST-RR	3753.1	851.1	0	8529.1	0.651	3.797	2.634	0.432	0.681
Remain-RR	3765.8	839.8	0	8530.4	0.788	3.591	1.646	0.437	0.678
LLF-RR	3765.9	802.6	0	8493.3	0.662	3.851	0.723	0.373	0.625
FOCS [2]	3767.9	657.7	0	8350.5	0.660	3.817	0.659	0.369*	0.544
SCOMMIT [1]	3767.9	668.8	0	8361.6	0.631	3.583	0.850	**0.358**	0.544
RI (κ=0.15)	3762.3	616.7	36.3	8340.2	0.686	3.727	1.138	0.391	0.532
RI-Q (κ=0.15)	3761.3	531.1	35.3	8252.5	0.665	3.890	1.120	0.389	0.484
POSKID (κ=0.15)	3762.5	523.7	34.3	8245.4	0.672	3.616	1.140	0.383	0.477
RI (κ=0.20)	3761.2	587.7	38.6	8312.4	0.671	3.696	1.261	0.389	0.516
RI-Q (κ=0.20)	3759.3	538.0	36.6	8258.9	0.651	3.619	1.058	0.373	0.480
POSKID(κ=0.20)	3756.0	506.8	36.7	8224.4*	0.653	3.691	1.094	0.377	**0.466**
RI (κ=0.25)	3756.1	587.8	40.0	8308.8	0.687	3.815	1.245	0.398	0.520
RI-Q (κ=0.25)	3762.1	534.3	36.1	8257.4	0.691	3.697	1.129	0.391	0.488
POSKID(κ=0.25)	3758.3	502.5	37.0	**8222.7**	0.678	3.919	0.981	0.389	0.469*

Table 4. Performance comparison with simulation strategy S_{future}. For the evaluation of "Total Cost" and "Dissatisfaction Score", the best and second-best results are highlighted in **bold** and marked with an asterisk (*), respectively. Cells highlighted in gray indicate results that rank in the lowest 40% for either total scores or dissatisfaction scores, excluding the scenario of "Uncoordinated".

Methods	Operating Cost				User Dissatisfaction				Overall
	Energy Charge (USD) (↓)	Penalty Charge (USD) (↓)	Incentive Cost (USD) (↓)	**Total Cost (USD) (↓)**	Infrequency Ratio (↓)	Moving Distance (km) (↓)	Time Difference (hr) (↓)	**Dissatisfaction Score (↓)**	**Penalty-Plus-Dissatisfaction Score (↓)**
Uncoordinated	3767.1	914.5	0	8606.5	0.212	0.650	0.271	0.101	0.550
S-RR	3761.7	725.6	0	8412.2	0.830	3.841	0.684	0.428	0.610
ST-RR	3754.2	873.2	0	8552.2	0.801	3.945	2.384	0.478	0.716
Remain-RR	3767.5	787.5	0	8479.8	0.869	4.903	2.264	0.529	0.695
LLF-RR	3762.9	720.9	0	8408.7	0.793	3.640	0.696	**0.409**	0.598
FOCS [2]	3768.0	701.3	0	8394.1	0.809	3.751	0.688	0.418*	0.592
SCOMMIT [1]	3767.9	676.0	0	8368.7	0.812	3.855	0.678	0.422	0.580
RI (κ=0.15)	3753.9	595.2	40.4	8314.3	0.756	3.711	1.424	0.423	0.537
RI-Q (κ=0.15)	3754.6	532.4	36.9	8248.8	0.779	3.942	1.085	0.427	0.505
POSKID (κ=0.15)	3753.7	513.0	36.7	**8228.2**	0.759	3.839	1.103	0.418	**0.489**
RI (κ=0.20)	3756.2	585.4	40.9	8307.4	0.805	3.953	1.394	0.447	0.543
RI-Q (κ=0.20)	3764.5	532.2	38.3	8259.8	0.778	3.836	0.996	0.421	0.501
POSKID(κ=0.20)	3760.6	522.2	37.4	8245.1*	0.785	3.838	1.048	0.425	0.498
RI (κ=0.25)	3756.4	585.6	41.5	8308.3	0.753	3.894	1.403	0.428	0.534
RI-Q (κ=0.25)	3761.5	536.6	38.5	8261.4	0.780	3.815	1.177	0.426	0.506
POSKID(κ=0.25)	3763.4	520.7	37.0	8245.9	0.771	3.799	1.045	0.419	0.494*

the lowest dissatisfaction scores in Table 3 and Table 4, respectively, but the differences compared to other methods are marginal. Remain-RR exhibits a higher dissatisfaction score under both simulation strategies $S_{history}$ and S_{future}, attributed to its recommendations not aligning well with users' preferences, indicated by a higher infrequency ratio. While *POSKID* may not secure the lowest dissatisfaction score, it remains competitive in Table 3 (with $\kappa = 0.20$) and Table 4 (with $\kappa = 0.15$). This indicates that *POSKID*, achieving the lowest total cost, still provides satisfactory charging arrangements to EV users, requiring only minor adjustments in their charging behaviors.

- In comparing penalty-plus-dissatisfaction scores, incentive-based methods (RI, RI-Q, and *POSKID*) outperform other baselines with lower scores. Notably, *POSKID* consistently outperforms RI and RI-Q in all κ settings. This underscores the importance of estimating the benefit score and determining the appropriate incentive to enhance users' willingness-to-accept (WTA). Results from Tables 3 and 4 show *POSKID* significantly lowers total costs with only a small amount of incentive cost while maintaining competitive user satisfaction. This highlights the practicality of *POSKID* in spatial-temporal charging scheduling tasks.

4.3 Individual Benefit Analysis

To demonstrate the benefits of our framework for each ICS, we investigate whether each ICS experiences higher charging revenue from EV users or pays a lower penalty charge after applying *POSKID*. Since the charging fee and electricity cost vary across regions, we primarily compare the uncoordinated scenario and *POSKID* by analyzing two key statistics: (i) the number of assigned charging requests and (ii) the amount of power exceeding the contracted capacity of each ICS.

Figure 5 presents a comparison of *POSKID* against the uncoordinated scenario, under varying κ values of 0.15 and 0.25, and using simulation strategies $S_{history}$ (Figure 5a) and S_{future} (Figure 5b). In this figure, lower x-values for an ICS (a node) indicate reduced exceeding power relative to the uncoordinated scenario, while higher y-values denote an increase in charging requests. Detailed statistics for each ICS under *POSKID* ($\kappa = 0.15$) using the strategy $S_{history}$, compared to the uncoordinated scenario, are presented in Figure 6. These analyses lead to several key observations as follows.

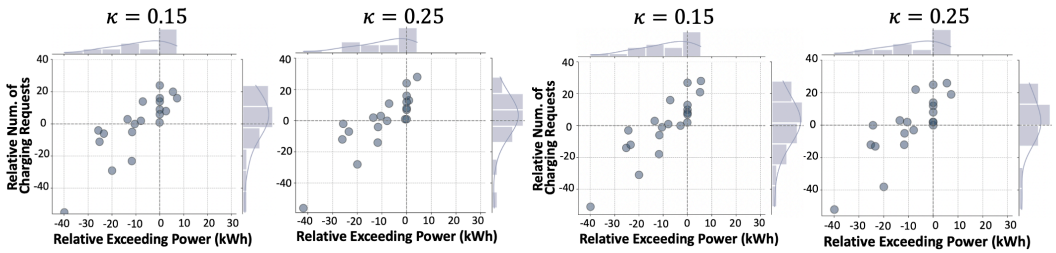

(a) Simulation Strategy $S_{history}$. (b) Simulation Strategy S_{future}.

Fig. 5. Relative Statistics of each ICS under different settings of κ. Each node in the figures represents an ICS. The x-axis and y-axis depict the disparity in exceeding power and the count of charging requests for an ICS between *POSKID* and the uncoordinated scenario, respectively.

- In Figure 5, we can observe that most of the nodes are located on the left side of the figures, indicating that the majority of ICSs have relatively lower exceeding power compared to the uncoordinated scenario. While some ICSs have decreased charging requests (located in the lower-left corner of the figures), those ICSs with higher reductions in charging requests still show a minimum decrease of 10 kWh in exceeding power. This reduction can save approximately USD 310 during the testing period of 7 days, based on the electricity price setting in Section 4.1.3.

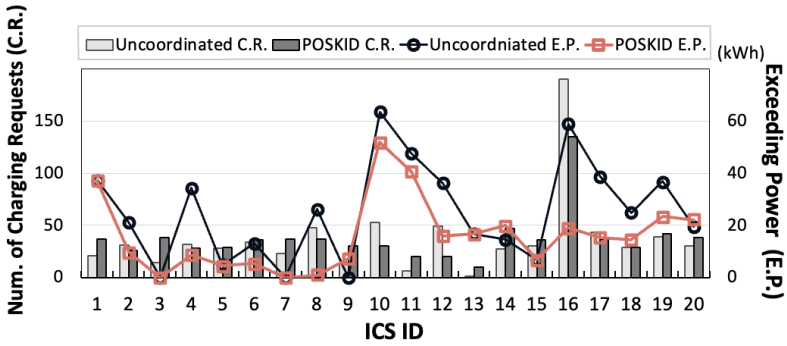

Fig. 6. The number of charging requests (C.R.) and the amount of exceeding power (E.P.) for each ICS under the uncoordinated scenario and *POSKID* ($\kappa = 0.15$) with simulation strategy $S_{history}$.

Additionally, some ICSs have higher exceeding power (located on the right side of the figures), but they are also assigned more charging requests, which can increase their revenues. Furthermore, as κ increases, some ICSs tend to converge towards the upper-left corner of the figures. This reveals that if EV users' acceptance probability is more influenced by the amount of provided incentives, *POSKID* can further enhance the benefits of ICSs through spatial-temporal charging scheduling.

- In Figure 6, it is evident that most of the ICSs exhibit lower exceeding power compared to the uncoordinated scenario. Furthermore, the less popular ICSs in the uncoordinated scenario can receive more charging requests with either decreased or nearly the same amounts of exceeding power (e.g., ICSs 1, 3, and 7). Conversely, the popular ICSs in the uncoordinated scenario can significantly reduce their exceeding power with only a slight decrease in charging requests (e.g., ICSs 8, 10, 12, and 16). These results demonstrate that our *POSKID* not only decreases the total costs but also brings benefits to each ICS individually.

4.4 Ablation Study and Parameter Sensitivity Analysis

The proposed *POSKID* consists of three main components: (i) personalized knowledge-based inference (P.I.), (ii) online candidate arrangement selection (O.S.), and (iii) interactive arrangement recommendation (I.R.). In Table 3 and Table 4, we demonstrate the necessity of the O.S. component by comparing them with baselines RI and RI-Q. In this subsection, we conduct an ablation study and parameter sensitivity analysis to evaluate the effectiveness of the two remaining components.

In Figure 7 and Figure 8, we present the penalty charges, dissatisfaction scores, and penalty-plus-dissatisfaction scores of *POSKID*, *POSKID* without I.R., and *POSKID* without P.I. under simulation strategies $S_{history}$ and S_{future}, respectively. Note that we implement *POSKID* without P.I. by substituting the personalized preference score $p^{v}_{n,\tau}$ (Eq. 11) with the historical visiting frequency ratio of user v at ICS n and time slot τ. Furthermore, we analyze the sensitivities of the embedding dimension applied in P.I. and the value of ϵ (Eq. 24) applied in I.R. under strategy $S_{history}$, as depicted in Figure 9. The embedding dimension influences the latent factors of EV users and ICSs, while the parameter ϵ directly affects the degree of exploitation of the optimal charging arrangements. Note that our default setting of the embedding dimension and the value of ϵ are 10 and 0.5, respectively. The following are the detailed observations:

- For the comparison of penalty charges (Figure 7a and Figure 8a), *POSKID* incurs much lower penalty charges than versions without I.R. and P.I., across all κ values. Notably, removing I.R. results in an increase in penalty charges to approximately USD 540 under both strategies. However, the absence of P.I. has a more pronounced impact on penalty charges under strategy S_{future} (Figure 8a) compared to strategy $S_{history}$ (Figure 7a). This observation suggests that when users'

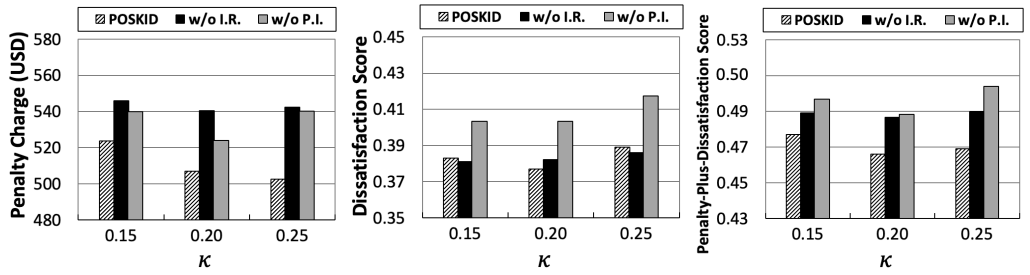

(a) Penalty Charge. (b) Dissatisfaction Score. (c) Penalty-Plus-Dissatisfaction.

Fig. 7. Ablation study of the interactive arrangement recommendation (I.R.) and the personalized knowledge-based inference (P.I.) with different values of κ under strategy S_{history}.

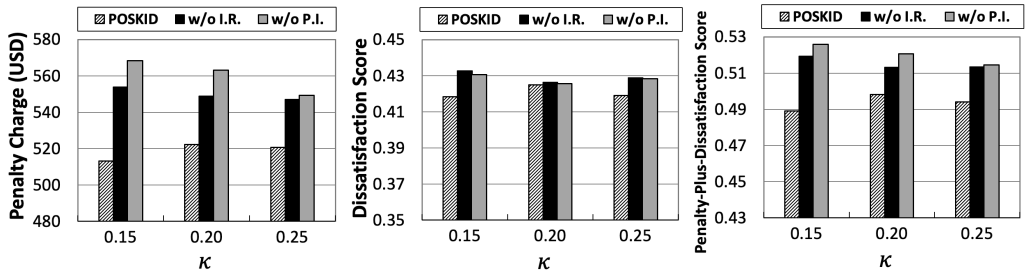

(a) Penalty Charge. (b) Dissatisfaction Score. (c) Penalty-Plus-Dissatisfaction.

Fig. 8. Ablation study of the interactive arrangement recommendation (I.R.) and the personalized knowledge-based inference (P.I.) with different values of κ under strategy S_{future}.

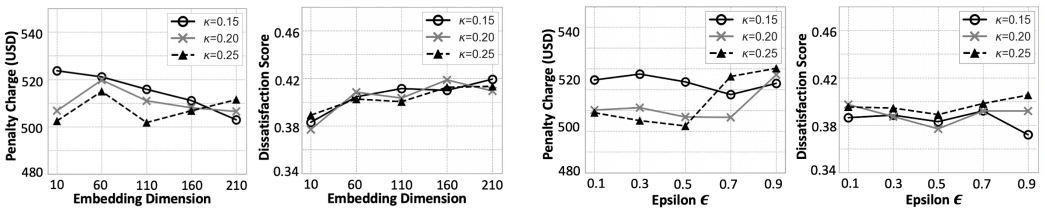

(a) Different embedding dimensions. (b) Different epsilon values (ϵ).

Fig. 9. The penalty charge and the dissatisfaction score of *POSKID* by varying the embedding dimension and the epsilon value (ϵ) under strategy S_{history}.

acceptance of recommended charging arrangements does not strictly follow their historical charging behaviors, employing personalized knowledge-based inference (P.I.) can more effectively reduce penalty charges by enhancing the success rate of recommendations.

- For the comparison of dissatisfaction scores (Figure 7b and Figure 8b), the complete *POSKID* model consistently achieves the lowest scores across most κ settings. Moreover, penalty-plus-dissatisfaction scores of *POSKID* are also the lowest under both strategies in Figure 7c and Figure 8c, highlighting the importance of including both I.R. and P.I. components. This underscores the effectiveness of our *POSKID* design.

- Figure 9 shows the performance of *POSKID* by setting the embedding dimension as {10, 60, 110, 160, 210} (Figure 9a) and the value of ϵ as {0.1, 0.3, 0.5, 0.7, 0.9} (Figure 9b). In Figure 9a, dissatisfaction scores for the three κ values exhibit minimal variation across different embedding dimensions. However, *POSKID* demonstrates consistent performance in penalty charges across all κ values only at the embedding dimension of 60, indicating that overly small or large embedding dimensions may result in unstable performance. In Figure 9b, setting ϵ to 0.9 (indicating a lower exploitation probability) leads to varied dissatisfaction scores across different κ values and generally results in higher penalty charges. This highlights the importance of exploiting the charging arrangement with the highest q-value, based on user feedback, to effectively address varying degrees of user acceptance influenced by the incentives offered.

5 RELATED WORKS

The design of our *POSKID* is closely related to two categories of EV charging management: (i) online EV charging problem and (ii) multiple charging stations management.

5.1 Online EV Charging Problem

Online charging decisions are often made with limited future information. Previous studies proposed online algorithms for EV charging in various scenarios. For example, Tang *et. al.* [35] suggested a coordinated charging algorithm to minimize costs. Zhao *et. al.* [45] explored competitive algorithms for EV charging to minimize grid electricity procurement. Guo *et. al.* [14] proposed an online algorithm based on linear programming to satisfy EV charging demand within power capacity. Some work [1] [32] scheduled EV charging based on on-arrival commitments. Alinia *et. al.* [1] devised scheduling algorithms for on-arrival commitment and deadline-constrained EVs. Sun *et. al.* [32] considered pricing to decide recommendations and charging schedules for sequential EV arrivals. Furthermore, some works addressed user charging satisfaction in different settings [24][44], where dissatisfaction captures users' preference for incomplete charging. Certain works [2][33] applied the knapsack problem in online EV charging, similar to our method, designing unit values for each charging request to determine scheduling priority. Additionally, the previous study [2] considers the highest price users are agreeable to offer to ensure their EV is charged before the requested time.

However, these studies primarily focus on scheduling EV charging to minimize costs, without inferring user acceptance of adjustments to their charging behaviors. In the real world, it is crucial to consider the users' willingness to accept (WTA) recommendations and strategies to enhance their willingness for successful EV scheduling. Therefore, an efficient approach is required to reduce charging station expenses considering users' preferences and their willingness to accept (WTA) using incentive strategies.

5.2 Multiple Charging Stations Management

The EV charging management in scenarios with multiple charging stations focuses on minimizing costs and maximizing user convenience. Several approaches have been proposed to address this challenge. Tian *et. al.* [37] utilize real-time GPS data mining to recommend charging stations for EV taxis. Guo *et. al.* [15] employ game theory to minimize travel time and queuing for EVs. Cao *et. al.* [5] propose a global aggregator that considers charging station conditions and EV charging reservations to make recommendations. Cung *et. al.* [7] design an optimization approach for minimizing charging costs and maximizing user convenience. Various other strategies, such as mobile edge computing (MEC) [4], model predictive control (MPC) [46], Lyapunov optimization [11], Markov Decision Problem [23], and cooperative multi-agent systems [29], have also been proposed to address different aspects of EV charging management.

Nevertheless, most of these studies mainly focus on where to charge (spatial scheduling), neglecting the optimal charging times (temporal scheduling). This limits flexibility in adjusting charging conditions flexibly across different times and could increase costs for charging stations. Furthermore, while some studies aim to reduce charging costs and time for EV users, they often overlook whether the charging stations match users' preferences and their willingness to adjust their charging behaviors. Moreover, they aim to minimize the overall operating costs, not ensuring benefits for each station within their system. These issues highlight our work, focusing on spatio-temporal charging scheduling, aiming to not only minimize overall operating costs but also ensure user preference by considering their willingness to accept scheduling. Additionally, our experiments confirm benefits for every involved ICS in our *POSKID*, revealing the practicality of *POSKID*.

6 CONCLUSION

In this paper, we propose the task of spatial-temporal charging scheduling among multiple charging stations in an online setting. The *POSKID* framework is introduced, which incorporates a personalized knowledge-based inference model to infer users' implicit charging preferences. Furthermore, an online candidate arrangement selection process is implemented, utilizing an explore-exploit strategy to dynamically make recommendation decisions based on users' feedback. Experimental results demonstrate that our *POSKID* framework achieves the lowest operating cost compared to other scheduling methods, while also ensuring users' charging satisfaction. The results further highlight the significant benefits that each charging station can derive from the application of *POSKID*, emphasizing its advantages in real-world deployments.

ACKNOWLEDGEMENT This paper was supported in part by National Science and Technology Council (NSTC), R.O.C., under Contract 112-2221-E-006-158, 113-2622-8-006-011-TD1 and 113-2221-E-006-203-MY2.

REFERENCES

[1] Bahram Alinia, Mohammad Hassan Hajiesmaili, and Noël Crespi. 2019. Online EV Charging Scheduling With On-Arrival Commitment. *IEEE Transactions on Intelligent Transportation Systems* 20 (2019), 4524–4537.

[2] Bahram Alinia, Mohammad Hassan Hajiesmaili, Zachary J. Lee, Noël Crespi, and Enrique Mallada. 2022. Online EV Scheduling Algorithms for Adaptive Charging Networks with Global Peak Constraints. *IEEE Transactions on Sustainable Computing* 7 (2022), 537–548.

[3] Arulampalam Atputharajah and Tapan Kumar Saha. 2009. Power system blackouts-literature review. In *2009 International Conference on Industrial and Information Systems (ICIIS)*. IEEE, 460–465.

[4] Yue Cao, Omprakash Kaiwartya, Y. Zhuang, Naveed Ahmad, Yan Lindsay Sun, and Jaime Lloret. 2019. A Decentralized Deadline-Driven Electric Vehicle Charging Recommendation. *IEEE Systems Journal* 13 (2019), 3410–3421.

[5] Yue Cao, Tong Wang, Omprakash Kaiwartya, Geyong Min, Naveed Ahmad, and Abdul Hanan Abdullah. 2018. An EV Charging Management System Concerning Drivers' Trip Duration and Mobility Uncertainty. *IEEE Transactions on Systems, Man, and Cybernetics: Systems* 48 (2018), 596–607.

[6] Dong Chen and David E. Irwin. 2017. SunDance: Black-box Behind-the-Meter Solar Disaggregation. *Proceedings of the Eighth International Conference on Future Energy Systems* (2017).

[7] Hwei-Ming Chung, Wen-Tai Li, Chau Yuen, Chao-Kai Wen, and Noël Crespi. 2018. Electric Vehicle Charge Scheduling Mechanism to Maximize Cost Efficiency and User Convenience. *IEEE Transactions on Smart Grid* 10 (2018), 3020–3030.

[8] CNET. 2023. *Electric Vehicle Sales Expected to Increase 35% in 2023*. https://www.cnet.com/roadshow/news/1-in-5-cars-sold-in-2023-predicted-to-be-electric-vehicles/

[9] Dundee City Council. 2018. *Electric Vehicle Charging Sessions Dundee*. https://www.drivedundeeelectric.co.uk/

[10] Soumaya Dahi and Sami Tabbane. 2013. Sigmoid utility function formulation for handoff reducing Access model in cognitive radio. *2013 13th International Symposium on Communications and Information Technologies (ISCIT)* (2013), 166–170.

[11] Fadi Elghitani and Ehab Fahmy El-Saadany. 2021. Efficient Assignment of Electric Vehicles to Charging Stations. *IEEE Transactions on Smart Grid* 12 (2021), 761–773.

[12] Miguel A. Fernández, Angel L. Zorita, Luis Angel García-Escudero, Oscar Duque, D. Morinigo, M. V. Riesco, and M. G. Munoz. 2013. Cost optimization of electrical contracted capacity for large customers. *International Journal of Electrical Power & Energy Systems* 46 (2013), 123–131.

[13] Sebastian Gottwalt, Wolfgang Ketter, Carsten Block, John Collins, and Christof Weinhardt. 2011. Demand side management—A simulation of household behavior under variable prices. *Energy Policy* 39 (2011), 8163–8174. https://api.semanticscholar.org/CorpusID:154703754

[14] Linqi Guo, Karl Fredrik Erliksson, and Steven H. Low. 2017. Optimal online adaptive electric vehicle charging. *2017 IEEE Power & Energy Society General Meeting* (2017), 1–5.

[15] Tianci Guo, Pengcheng You, and Zaiyue Yang. 2017. Recommendation of geographic distributed charging stations for electric vehicles: A game theoretical approach. *2017 IEEE Power & Energy Society General Meeting* (2017), 1–5.

[16] William L. Hamilton, Zhitao Ying, and Jure Leskovec. 2017. Inductive Representation Learning on Large Graphs. In *NIPS*.

[17] Ying-Chao Hung and George Michailidis. 2019. Modeling and Optimization of Time-of-Use Electricity Pricing Systems. *IEEE Transactions on Smart Grid* 10 (2019), 4116–4127. https://api.semanticscholar.org/CorpusID:115437455

[18] International Energy Agency (IEA). 2023. *Global EV Outlook 2023*. https://www.iea.org/reports/global-ev-outlook-2023

[19] Cheng-Peng Kuan and Kuu young Young. 1998. Reinforcement Learning and Robust Control for Robot Compliance Tasks. *Journal of Intelligent and Robotic Systems* 23 (1998), 165–182.

[20] Matthias Kühnbach, Judith Stute, and Anna-Lena Klingler. 2021. Impacts of avalanche effects of price-optimized electric vehicle charging-Does demand response make it worse? *Energy Strategy Reviews* 34 (2021), 100608.

[21] Zachary J. Lee, George S. Lee, Ted Lee, Cheng Jin, Rand Lee, Zhi Low, Daniel Chang, Christine Ortega, and Steven H. Low. 2020. Adaptive Charging Networks: A Framework for Smart Electric Vehicle Charging. *IEEE Transactions on Smart Grid* 12 (2020), 4339–4350.

[22] Hepeng Li, Zhiqiang Wan, and Haibo He. 2020. Constrained EV Charging Scheduling Based on Safe Deep Reinforcement Learning. *IEEE Transactions on Smart Grid* 11 (2020), 2427–2439.

[23] Hai Lin, Xiang Lin, Houda Labiod, and Lin Chen. 2022. Toward Multiple-Phase MDP Model for Charging Station Recommendation. *IEEE Transactions on Intelligent Transportation Systems* 23 (2022), 10583–10595.

[24] Qiulin Lin, Hanling Yi, and Minghua Chen. 2022. Minimizing Cost-Plus-Dissatisfaction in Online EV Charging Under Real-Time Pricing. *IEEE Transactions on Intelligent Transportation Systems* 23 (2022), 12464–12479.

[25] Silvano Martello and Paolo Toth. 1990. Knapsack Problems: Algorithms and Computer Implementations.

[26] Clayton Miller. 2012. ENERNOC commercial building dataset. http://cargocollective.com/buildingdata/100-EnerNOC-Commercial-Buildings.

[27] Steffen Rendle, Christoph Freudenthaler, Zeno Gantner, and Lars Schmidt-Thieme. 2009. BPR: Bayesian Personalized Ranking from Implicit Feedback. *ArXiv* abs/1205.2618 (2009).

[28] Barbara Rosado, Ricardo Torquato, Bala Venkatesh, Hoay Beng Gooi, Walmir Freitas, and Marcos J. Rider. 2020. Framework for optimizing the demand contracted by large customers. *IET Generation, Transmission & Distribution* (2020).

[29] Can Berk Saner, Anupam Trivedi, and Dipti Srinivasan. 2022. A Cooperative Hierarchical Multi-Agent System for EV Charging Scheduling in Presence of Multiple Charging Stations. *IEEE Transactions on Smart Grid* 13 (2022), 2218–2233.

[30] Charles Satterfiled and Nick Nigro. 2020. *Public EV Charging Business Models for Retail Site Hosts*. https://atlaspolicy.com/wp-content/uploads/2020/04/Public-EV-Charging-Business-Models-for-Retail-Site-Hosts.pdf

[31] Devavrat Shah and Qiaomin Xie. 2018. Q-learning with Nearest Neighbors. In *NeurIPS*.

[32] Bo Sun, Tongxin Li, Steven H. Low, and Danny Hin-Kwok Tsang. 2020. ORC: An Online Competitive Algorithm for Recommendation and Charging Schedule in Electric Vehicle Charging Network. *Proceedings of the Eleventh ACM International Conference on Future Energy Systems* (2020).

[33] Bo Sun, Ali Zeynali, Tongxin Li, Mohammad Hassan Hajiesmaili, Adam Wierman, and Danny Hin-Kwok Tsang. 2020. Competitive Algorithms for the Online Multiple Knapsack Problem with Application to Electric Vehicle Charging. *Proceedings of the ACM on Measurement and Analysis of Computing Systems* 4 (2020), 1 – 32.

[34] Hengky Susanto. 2014. From Self-Regulate to Admission Control in Real-Time Traffic Environment. *2014 IEEE 28th International Conference on Advanced Information Networking and Applications* (2014), 9–16.

[35] Wanrong Tang, Suzhi Bi, and Ying Jun Angela Zhang. 2013. Online Coordinated Charging Decision Algorithm for Electric Vehicles Without Future Information. *IEEE Transactions on Smart Grid* 5 (2013), 2810–2824.

[36] FreeWire Technologies. 2020. *What's the Difference Between EV Charging Levels?* https://freewiretech.com/difference-between-ev-charging-levels/

[37] Zhiyong Tian, Taeho Jung, Yi Wang, Fan Zhang, Lai Tu, Cheng-Zhong Xu, Chen Tian, and Xiang-Yang Li. 2016. Real-Time Charging Station Recommendation System for Electric-Vehicle Taxis. *IEEE Transactions on Intelligent Transportation Systems* 17 (2016), 3098–3109.

[38] Lo Pang-Yun Ting, Po-Hui Wu, Hsiu-Ying Chung, and Kun-Ta Chuang. 2022. An Incentive Dispatch Algorithm for Utilization-Perfect EV Charging Management. In *Pacific-Asia Conference on Knowledge Discovery and Data Mining*.

[39] Ran Wang, Ping Wang, and Gaoxi Xiao. 2016. Two-Stage Mechanism for Massive Electric Vehicle Charging Involving Renewable Energy. *IEEE Transactions on Vehicular Technology* 65 (2016), 4159–4171.

[40] Stephen D. Wong, Susan A. Shaheen, Elliot W. Martin, and Robert Uyeki. 2023. Do incentives make a difference? Understanding smart charging program adoption for electric vehicles. *Transportation Research Part C: Emerging Technologies* (2023). https://api.semanticscholar.org/CorpusID:258147952

[41] Keyulu Xu, Weihua Hu, Jure Leskovec, and Stefanie Jegelka. 2019. How Powerful are Graph Neural Networks?. In *International Conference on Learning Representations*. https://openreview.net/forum?id=ryGs6iA5Km

[42] Qin Yan, Bei Zhang, and Mladen Kezunovic. 2019. Optimized Operational Cost Reduction for an EV Charging Station Integrated With Battery Energy Storage and PV Generation. *IEEE Transactions on Smart Grid* 10 (2019), 2096–2106.

[43] Bishan Yang, Wen tau Yih, Xiaodong He, Jianfeng Gao, and Li Deng. 2014. Embedding Entities and Relations for Learning and Inference in Knowledge Bases. *CoRR* abs/1412.6575 (2014).

[44] Hanling Yi, Qiulin Lin, and Minghua Chen. 2019. Balancing Cost and Dissatisfaction in Online EV Charging under Real-time Pricing. *IEEE INFOCOM 2019 - IEEE Conference on Computer Communications* (2019), 1801–1809.

[45] Shizhen Zhao, Xiaojun Lin, and Minghua Chen. 2015. Peak-minimizing online EV charging: Price-of-uncertainty and algorithm robustification. *2015 IEEE Conference on Computer Communications (INFOCOM)* (2015), 2335–2343.

[46] Yu Zheng, Yue Song, David. J. Hill, and Ke Meng. 2019. Online Distributed MPC-Based Optimal Scheduling for EV Charging Stations in Distribution Systems. *IEEE Transactions on Industrial Informatics* 15 (2019), 638–649.

[47] Yunhong Zhou, Deeparnab Chakrabarty, and Rajan M. Lukose. 2008. Budget Constrained Bidding in Keyword Auctions and Online Knapsack Problems. In *WINE*.